Supporting Information

Armstrong et al. 10.1073/pnas.1109709109

SI Text

Materials and Methods ***Red-green color correction and alignment*** A two-dimensional lookup table routine, implemented in Matlab (Mathworks Inc.), was used to spatially register the coordinates of quantum dots tracked through sequences of red and green images. The lookup table was first constructed by simultaneously acquiring red and green images of a 0.19 μm multicolored fluorescent bead (Ultra Rainbow Particles; Spherotech) on a glass cover slip. A piezoelectric x-y translation stage was used to move the bead around the microscope's field of view in a grid pattern with 1.7 μm spacing. An image was acquired with the bead at each point in the grid, and the series was merged into a single image for each channel (Fig. S9*A*).

A particle image velocimetry routine (1) (mpiv toolbox by Nobuhito Mori, distributed under GNU public license) was used, which was developed for fluid flow applications to determine the displacement of particles between two images by 2D cross-correlation. The cross-correlation involved taking a 120 pixel, square window in both the red and green images and rastering these windows simultaneously through the two images with 85% overlap for one window position to the next. This routine created an array of 126 vectors defining the correction offsets required at each location within the red channel image to match up with the green channel image (Fig. S9*B*). This array was then cubically interpolated to provide offsets for each pixel in both the horizontal and vertical dimensions (Fig. S9*C*). The procedure was repeated nineteen times with different grid images, and the standard deviations of horizontal and vertical offsets were used as a measure of local uncertainty of the lookup table, with greater standard deviations indicative of greater uncertainty (Fig. S9*D*).

Each dual-colored FLB-myoV head position trace was then aligned by taking the x and y coordinates of the red quantum dot-labeled head at each time point and correcting its position relative to the green quantum dot-labeled head by the appropriate horizontal and vertical correction offsets (Fig. S9*C*) with subpixel resolution.

1. Michalek AJ, Buckley MR, Bonassar LJ, Cohen I, & Iatridis JC (2009) Measurement of local strains in intervertebral disc anulus fibrosus tissue under dynamic shear: contributions of matrix fiber orientation and elastin content. *J Biomech* 42(14):2279–2285.

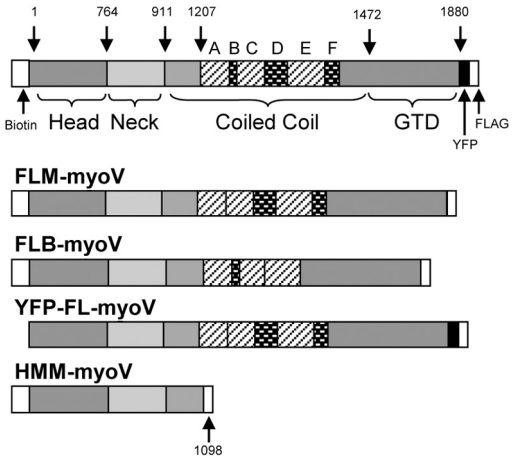

Fig. S1. MyoV constructs. (*Top*) The full-length myoV transcript containing all exons, an N-terminal biotin tag for conjugation with streptavidin-Qdots, and a C-terminal YFP and FLAG tag for purification. Alternatively spliced exons *A*–*G* are labeled. The melanocyte splice variant (FLM-myoV) expresses exons ACDEF without the YFP whereas the brain splice variant (FLB-myoV) expresses exons ABCE without the YFP. A FLM-myoV YFP construct (YFP-FLM-myoV) without the N-terminal biotin was used as a control for artifacts potentially created by the addition of a Qdot to the N-terminus of the motor. The HMM-myoV construct is truncated at amino acid 1098, prior to the PEST site within the coiled-coil tail.

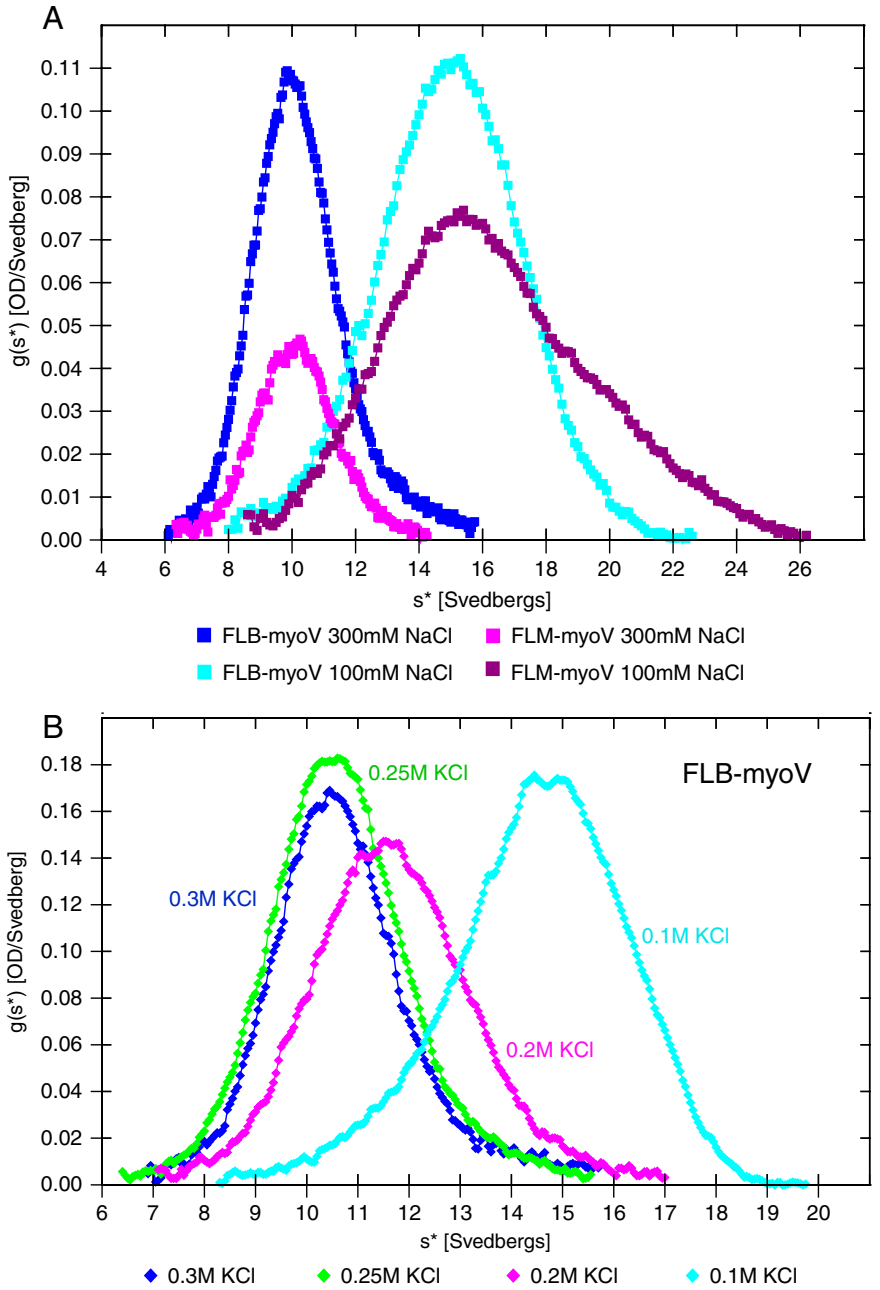

Fig. S2. Characterization of full-length constructs by analytical ultracentrifugation. (*A*) At 100 mM NaCl both FLB-myoV (cyan) and FLM-myoV (burgundy) adopt the folded conformation which sediments at approximately 15 S. At 300 mM NaCl, both isoforms form an extended conformation that sediments at approximately 10 S (FLB-myoV, blue; FLM-myoV, magenta) Buffer: 10 mM Hepes pH 7.4, 1 mM EGTA and DTT, 0.1 M, or 0.3 M NaCl. (*B*) Sedimentation of FLB-myoV as a function of KCl concentration shows that the molecule is primarily extended at 0.2 M KCl. Sedimentation values are: 14.8 S (0.1 M KCl); 11.5 S (0.2 M KCl); 10.5 S (0.25 M KCl); 10.5 S (0.3 M KCl). The buffer used for these experiments is identical to that used for the single-molecule studies (25 mM Imidazole pH 7.4, 4 mM $MgCl_2$, 1 mM EGTA and DTT, KCl at 0.1 M, 0.2 M, 0.25 M, or 0.3 M).

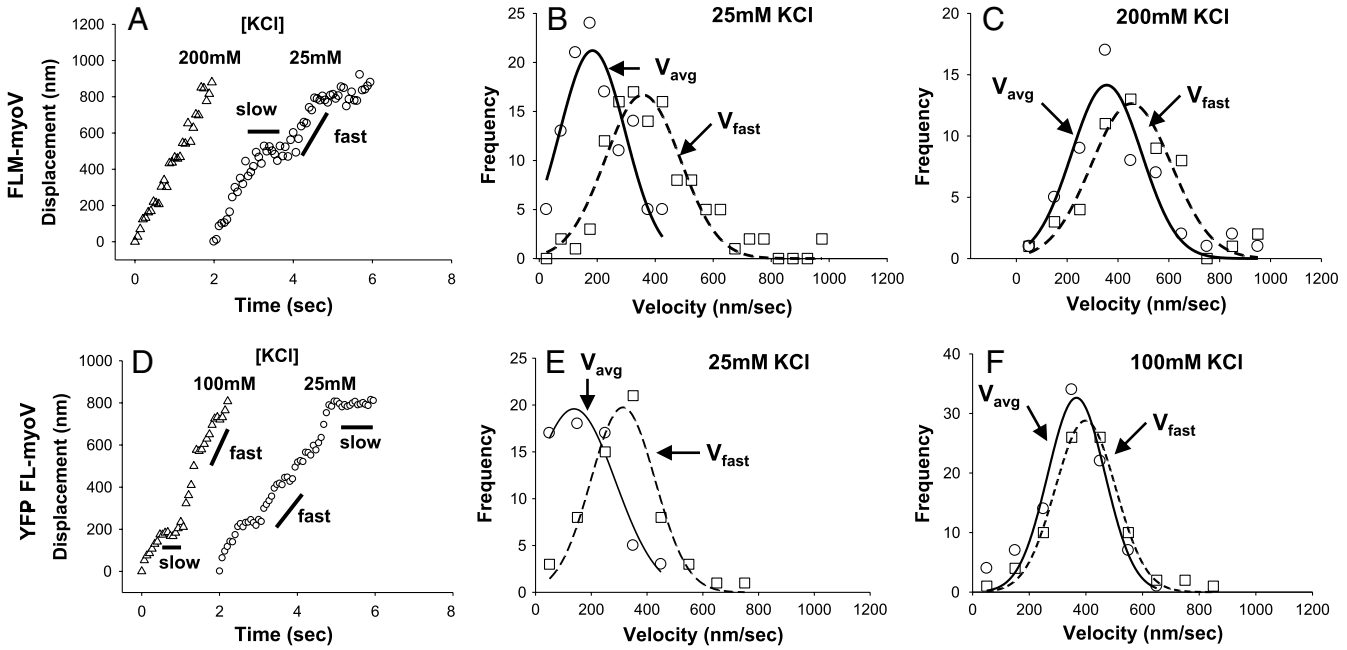

Fig. S3. Displacement versus time and velocity histograms as a function of ionic strength for FLM-myoV and YFP-FL-myoV. Typical displacement versus time traces at 100 mM or 200 mM KCl (as indicated, triangles) and 25 mM KCl (circles) at 1 mM ATP for the FLM-myoV (*A*) and YFP-FL-myoV (*D*). Solid lines indicate the fast and slow periods of processive movement Velocity histograms for FLM-myoV and YFP-FL-myoV at 25 mM KCl (*B*, *E*, respectively) and 200 mM or 100 mM KCl (*C*, *F*, respectively). Circles represent V_{avg} and squares represent V_{fast}.

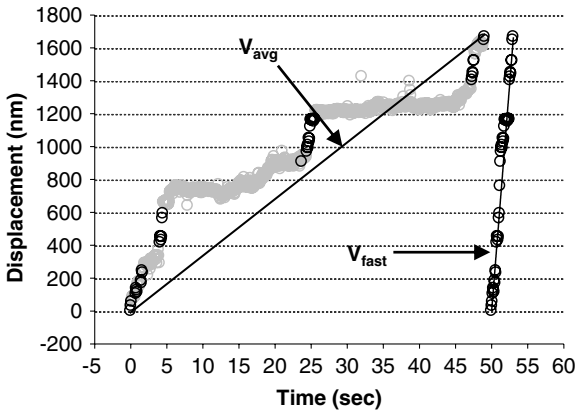

Fig. S4. Method for eliminating periods of slow processive motion from FL-myoV displacement trajectories. Typical displacement vs. time trace for FLB-myoV (left) at 25 mM KCl with periods of slow processive motion indicated as gray circles. The adjusted trace with the slow periods removed to estimate V_{fast} is shown on the right. The average velocity (line = V_{avg}) calculated as total distance traveled divided by total travel time for this trace gives a value of 22 nm/s while the regression through the adjusted trace gives a V_{fast} of 552 nm/s.

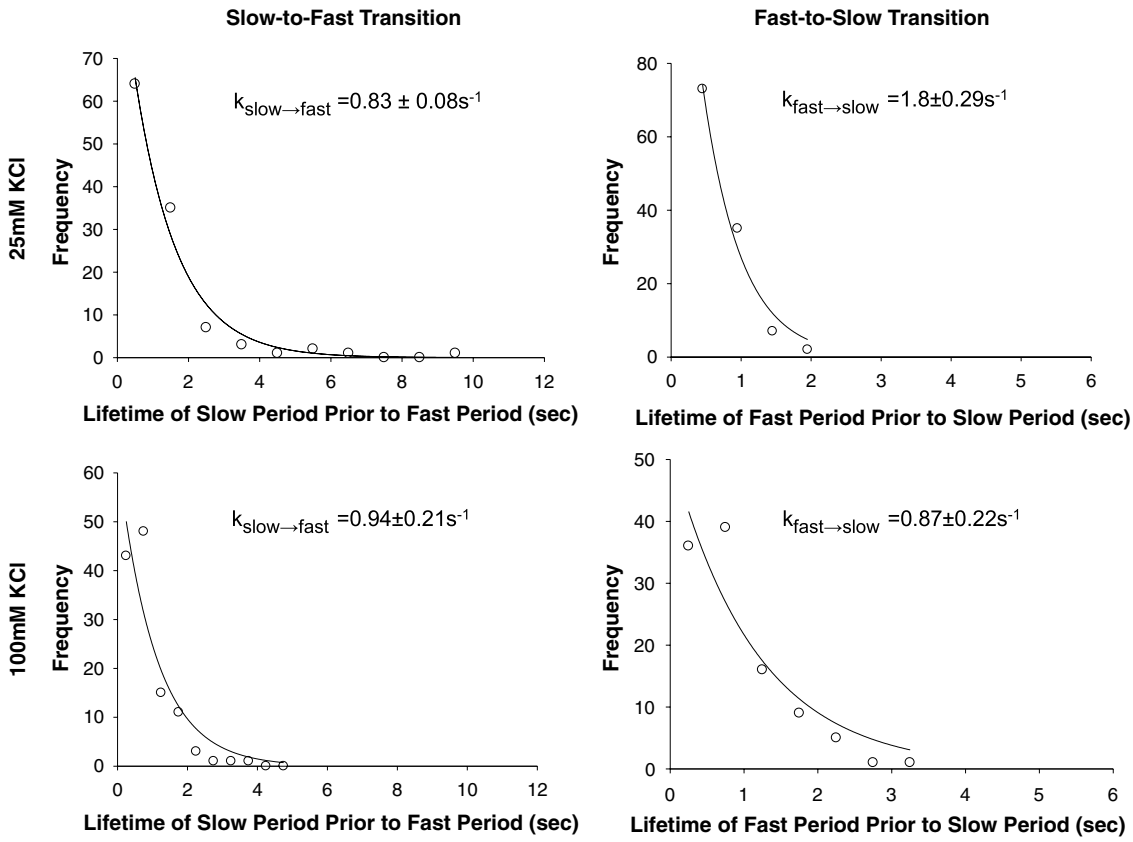

Fig. S5. Transition rates between periods of slow and fast processivity at 25 and 100 mM KCl. Lifetime histograms of the duration the motor spends in either the slow period prior to a fast processive period (*Left*) or in the fast period prior to switching to a slow processive period (*Right*). Histograms were fitted to an exponential to derive rate constants for the fit as shown on the graphs as mean ± standard error of the estimate.

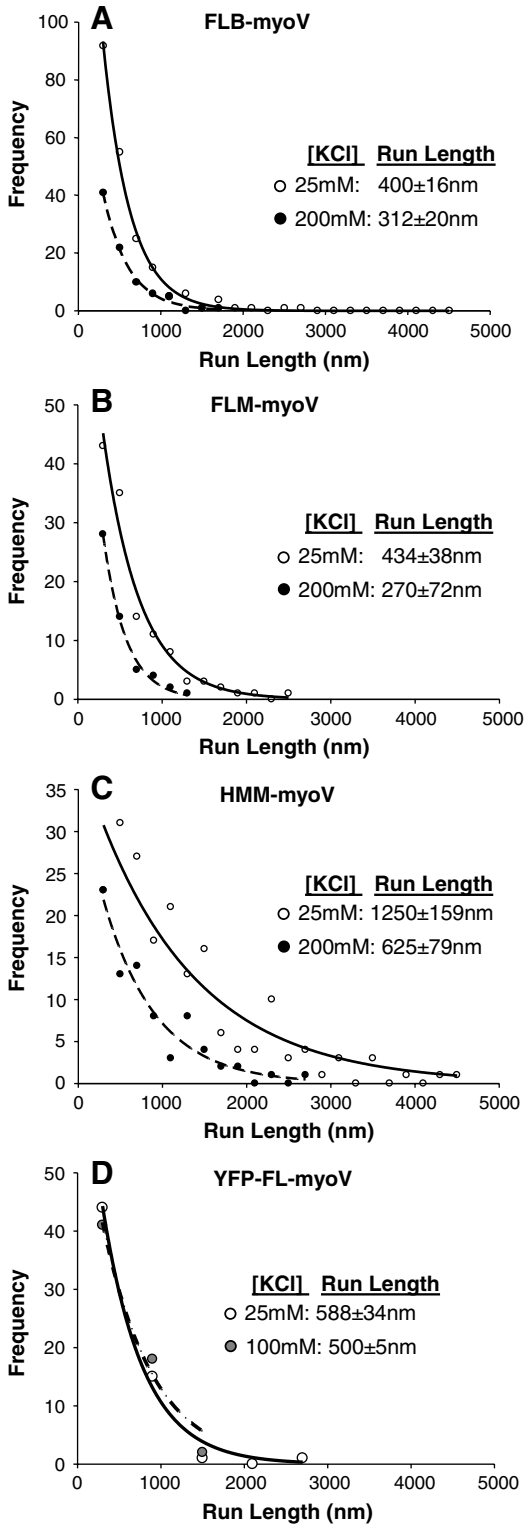

Fig. S6. Run length frequency histograms at 1 mM ATP. Run length frequency histograms for FLB-myoV (*A*), FLM-myoV (*B*), HMM-myoV (*C*), and YFP-FL-myoV (*D*) at 25 mM KCl (open circles), 200 mM KCl (closed circles), and 100 mM KCl for the YFP-FL-myoV (gray circles). Data were fit to an exponential decay and characteristic run lengths reported as 1/decay constant ± S.E.

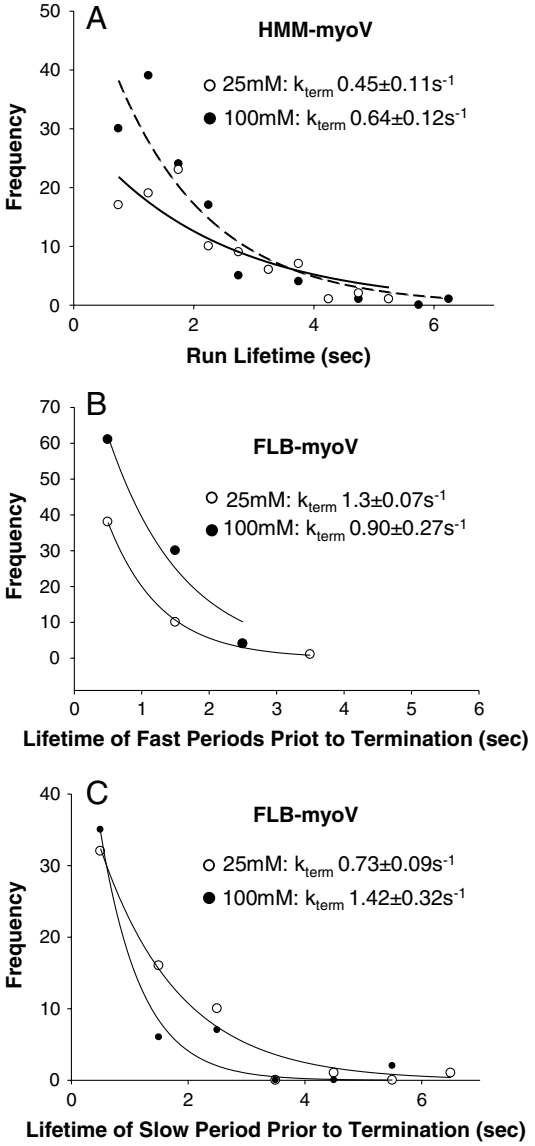

Fig. S7. Frequency histogram of HMM-myoV run lifetimes prior to termination at 25 mM ($n = 95$) (open circles) and 100 mM ($n = 75$) (closed circles) KCl. Distributions were fitted to an exponential decay and termination rates (k_{term}) reported as decay constant ± S.E. Frequency histograms of lifetimes for periods of V_{fast} (*C*) and V_{slow} (*D*) prior to termination for FLB-myoV and analyzed as in B to estimate termination rates from the fast and slow processive periods at 25 mM ($n > 41$) (open circles) and 100 mM ($n > 30$) (closed circles) KCl.

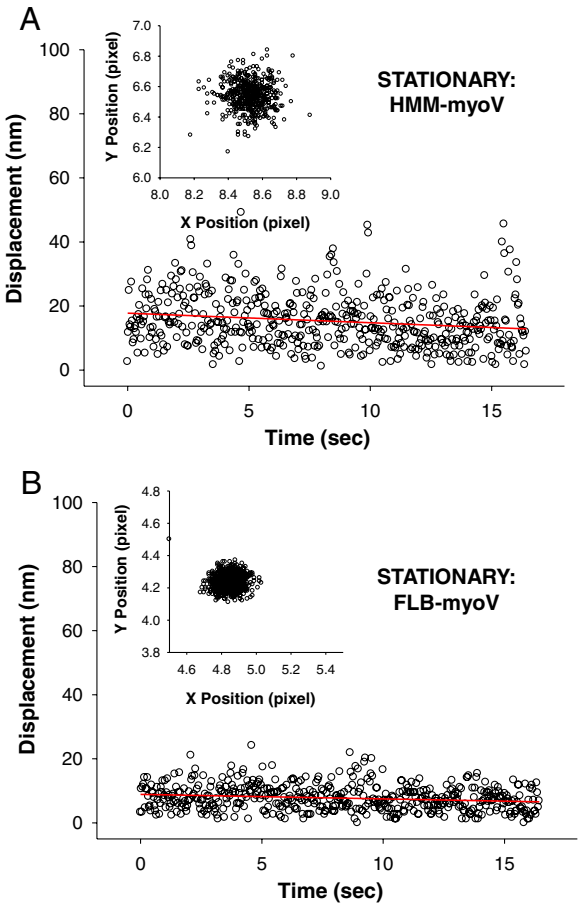

Fig. S8. Positional and displacement characterization of stationary HMM-myoV and FLB-myoV. (*A*) Displacement versus time trace for a stationary HMM-myoV obtained by tracking the *x*,*y* position (*Inset*) in pixels (117 nm/pixel) of the Qdot attached to the one of the motor's heads. No detectable steps were observed confirming that these nonmotile HMM-myoV are truly stationary. Red line is linear regression through the entire trace. The standard deviation of the Qdot position in the x-axis was 10 nm. (*B*) Displacement versus time trace for a stationary FLB-myoV obtained by tracking the *x*,*y* position (*Inset*) in pixels (117 nm/pixel) of the Qdot attached to the one of the motor's heads. No detectable steps were observed confirming that these nonmotile FLB-myoV are truly stationary and distinct from the stepping pattern observed during slow periods of processive motion. Red line is linear regression through the entire trace. The standard deviation of the Qdot position in the x-axis was 7 nm.

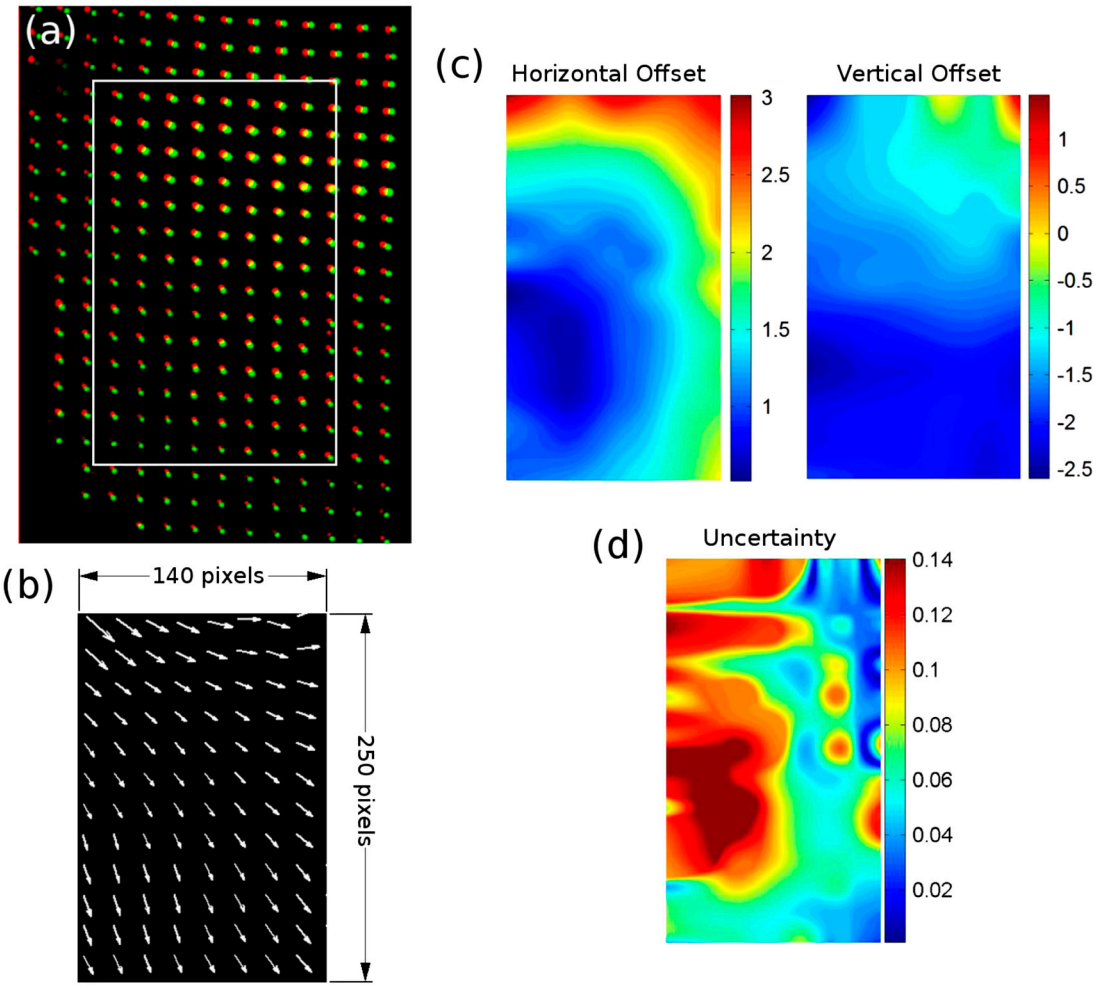

Fig. S9. Image color correction maps. (*A*) Multicolored fluorescent beads were simultaneously imaged in red and green and then merged with brightness and contrast adjusted for clarity. (*B*) A two dimensional correlation routine was used to generate a field of displacement vectors within the area indicated by the white box in (*A*). (*C*) The vector field in (*B*) was interpolated into horizontal offset and vertical offset lookup tables, which define the number of pixels (color bar) by which the red image must be offset to align with the green. (*D*) The procedure in (*A*–*C*) was repeated with nineteen different multicolored images, and the standard deviations of horizontal and vertical offsets were calculated as a measure of uncertainty, with greater standard deviations indicative of greater uncertainty.

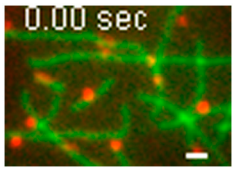

Movie S1. FLB-myoV is predominantly bound to and stationary on actin at low ionic strength (25 mM KCl) and 1 mM ATP. The majority of Qdot-labeled FLB-myoV (red) are stationary on actin filaments (green) at 25 mM KCl and 1 mM MgATP. However, two motors near the center of the field do move processively on actin for a short distance even though the full-length motor should be inhibited under these experimental conditions. The scale bar represents 1 μm. The original video was captured for 14.5 s (video playback speed is 2×).

Movie S1 (AVI)

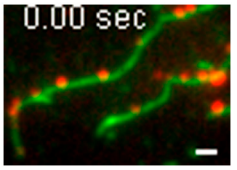

Movie S2. HMM-myoV moves processively along actin filaments at low ionic strength (25 mM KCl) and 1 mM ATP. Qdot-labeled HMM-myoV (red) are seen moving along actin filaments (green) at 25 mM KCl and 1 mM MgATP. In contrast to the full-length motors (see Movie S1), nearly all of the actin-associated motors are processive. The scale bar represents 1 μm. The original video was captured for 29.4 s (video playback speed is 2×).
Movie S2 (AVI)

Movie S3. FLB-myoV moves processively along actin at low ionic strength (25 mM KCl) and 1 mM ATP. A single Qdot-labeled FLB-myoV (red) is seen moving along an actin filament (green). As described in the text, this processive motion can be broken up in to periods of fast and slow movement. The scale bar represents 1 μm. The original video was captured for 49.5 s (video playback speed is 4×).
Movie S3 (AVI)

Movie S4. HMM-myoV moves processively along actin at low ionic strength (25 mM KCl) and 1 mM ATP. Two Qdot-labeled HMM-myoV (red) are seen moving along an actin filament (green). In contrast to FLB-myoV, HMM-myoV moves at a constant velocity throughout the entire trajectory. The scale bar represents 1 μm. The original video was captured for 9.5 s (video playback speed is 4×).
Movie S4 (AVI)